Pharm Res (2015) 32:167–179
DOI 10.1007/s11095-014-1453-9

RESEARCH PAPER

Probing the Effects of Experimental Conditions on the Character of Drug-Polymer Phase Diagrams Constructed Using Flory-Huggins Theory

Conor Donnelly • Yiwei Tian • Catherine Potter • David S. Jones • Gavin P. Andrews

Received: 25 February 2014 / Accepted: 2 July 2014 / Published online: 30 July 2014

ABSTRACT

Purpose Amorphous drug-polymer solid dispersions have been found to result in improved drug dissolution rates when compared to their crystalline counterparts. However, when the drug exists in the amorphous form it will possess a higher Gibb's free energy than its associated crystalline state and can recrystallize. Drug-polymer phase diagrams constructed through the application of the Flory Huggins (F-H) theory contain a wealth of information regarding thermodynamic and kinetic stability of the amorphous drug-polymer system. This study was aimed to evaluate the effects of various experimental conditions on the solubility and miscibility detections of drug-polymer binary system.

Methods Felodipine (FD)-Polyvinylpyrrolidone (PVP) K15 (PVPK15) and FD-Polyvinylpyrrolidone/vinyl acetate (PVP/VA64) were the selected systems for this research. Physical mixtures with different drug loadings were mixed and ball milled. These samples were then processed using Differential Scanning Calorimetry (DSC) and measurements of melting point (T_{end}) and glass transition (T_g) were detected using heating rates of 0.5, 1.0 and 5.0°C/min.

Results The melting point depression data was then used to calculate the F-H interaction parameter (χ) and extrapolated to lower temperatures to complete the liquid–solid transition curves. The theoretical binodal and spinodal curves were also constructed which were used to identify regions within the phase diagram. The effects of polymer selection, DSC heating rate, time above parent polymer T_g and polymer molecular weight were investigated by identifying amorphous drug miscibility limits at pharmaceutically relevant temperatures.

Conclusion The potential implications of these findings when applied to a non-ambient processing method such as Hot Melt Extrusion (HME) are also discussed.

C. Donnelly • Y. Tian • C. Potter • D. S. Jones • G. P. Andrews (✉)
The Drug Delivery and Biomaterials Group, School of Pharmacy
Medical Biology Centre, Queen's University, 97 Lisburn Road, BT9 7BL
Belfast, Northern Ireland, UK
e-mail: g.andrews@qub.ac.uk

KEY WORDS flory-huggins theory · phase diagrams · solid dispersions

INTRODUCTION

It is well accepted that high throughput screening (HTS) within drug discovery programmes has led to a significant increase in the number of poorly water-soluble drugs within development pipelines (1). Finding possible solutions to overcome this issue is a major challenge facing the pharmaceutical industry. At present, it is estimated that 70% of new chemical entities possess limited aqueous solubility and approximately 40% of currently marketed oral drug products are considered practically insoluble (<100 μg/ml) (2,3). Poor aqueous solubility of new drug candidates presents many problems during product development. For example, dissolution rate is limited and thus oral bioavailability is often low. This may be addressed via dose escalation; however this common approach is sub-optimal since it may increase local toxicity, hence reducing patient compliance. Moreover, drug product manufacture via conventional methods is not easily achieved when drug/excipient ratio is high, particularly when the drug possesses poor powder flow properties and/or compactability. Poor aqueous solubility also presents significant challenges when conducting important *in vitro* cell culture assays that are used to provide information on efficacy, membrane permeation and genotoxicity (4).

Many different methods have been utilized to address the issue of poor aqueous solubility including particle size reduction, amorphisation, crystal modification and self-emulsification. Amorphous solids have received particular attention, most probably due to the significant increase in solubility that may be achieved relative to the crystalline form of the drug (5). Amorphous drug forms possess a higher internal energy and specific volume relative to the crystalline form and it is these characteristics that can lead to enhanced

drug solubility and improved bioavailability for BCS class II drugs (6). In addition, amorphous drug forms do not require energy to disrupt a regular crystalline structure; hence the dissolution rate may also be improved (7). However, the high energy state associated with the amorphous form and the tendency to recrystallize is a principle concern and one of the key reasons behind the lack of marketed amorphous solid dispersions (8). Amorphous drugs can be stabilized by preparation of an amorphous solid dispersion (ASD), in which the drug is embedded in a polymeric carrier. Spray drying, melt mixing, melt extrusion, ball milling, injection moulding, lyophilisation and use of supercritical fluids can all be used to prepare ASD (9). Although the literature contains a significant volume of information detailing the development of ASD using different polymers and processes, most of the approaches described have been empirical, and in particular, the rationale for the selection of polymeric excipients is unclear. Moreover, there is limited information describing the stability of formulated ASD from a thermodynamic viewpoint.

In order to address this deficit, it is obvious that a greater understanding of the formulation and pharmaceutical processing of ASD are required to ensure that stable solid dispersions may be both predicted and prepared. Some very recent, and interesting research articles go some way to address this problem (10–15). The stability of amorphous solid dispersions has been linked to drug-polymer miscibility (16,17). Therefore, gaining further knowledge on miscibility limits; the amount of amorphous drug that can be incorporated in an amorphous carrier before the process of phase separation occurs would be extremely beneficial when applied to, specific preparation/manufacturing techniques. This would allow one to better understand how drug loading and temperature affect the thermodynamic stability of ASD. One potential solution to determine the limit of miscibility is the construction of thermodynamic drug-polymer phase diagrams based the Flory Huggins (FH) theory (14,18). The creation of drug-polymer phase diagrams is a growing area of interest with a number of important articles published recently (14,19). Our group have recently described a small-scale thermal method that can be used to establish temperature/composition phase diagrams (11). This may allow rapid screening of drug-polymer combinations in the context of phase separation. Using drug-polymer phase diagrams, a wealth of information with regard to the stability of amorphous solid dispersions including the liquid–solid phase boundary as well as the binodal and spinodal decomposition boundaries may be rapidly established. Using such an approach, will certainly not answer all questions regarding the efficacy of a specific polymer for stabilising ASD, but will allow for comparison of the temperature effects of boundary regions between metastable and unstable for different drug-polymer platforms (20,21). Currently, we understand that drug-polymer solid dispersions located beneath the spinodal curve possess a Gibb's free energy that is higher for the homogeneously mixed state, than that of the two individual phase separated states. A spontaneous phase separation will be observed, referred to as spinodal decomposition (22). The metastable region exists between the binodal and spinodal curves, a region wherein the system is stable to small fluctuations but unstable with respect to large fluctuation. Moreover, the width of the miscibility gap provides useful information in regard to the physical stability of amorphous solid dispersions and could be used during pre-formulation to facilitate selection of appropriate polymers and temperatures for processing and storage (from a thermodynamic perspective).

Previously our group has published a number of articles describing the construction and use, of temperature/composition phase diagrams, for drug-polymer systems of pharmaceutical interest (11,20). Our aim was to establish a rapid, screening method to better understand drug-polymer phase behaviour so that we could rationally select candidate polymers for melt extrusion of ASD. Achieving equilibrium during rapid small-scale DSC experiments is extremely difficult due to the high viscosity and long relaxation times associated with high molecular weight polymer chains. This limits diffusion of drug into the polymeric matrix during experimental timescales such that achieving equilibrium drug saturation is difficult (12). In this study, our aim was to investigate the effects of experimental conditions on melting endpoint of drug-polymer physical mixtures that are used to determine temperature/composition phase behaviour. This will allow us to better understand how the timescale of experimental observation influences the liquid–solid line, spinodal decomposition curve and the miscibility gap between drug and polymer. To do so, we have used felodipine as a model BCS class II drug and two pharmaceutically relevant polymeric excipients Polyvinylpyrrolidone (PVP) and Polyvinylpyrrolidone/vinyl acetate (PVP/VA64), to probe the effect of DSC heating rate, time above the glass transition temperature (T_g) and PVP molecular weight, upon the character of temperature/composition phase diagrams.

MATERIALS AND METHODS

Materials

Felodipine (FD) (Molecular weight, Mw = 384.26 g/mol) was purchased from Taresh Ltd. (Down, UK) and used without further purification. Polyvinylpyrrolidone (PVP) K15 (Mw = 10,000 g/mol) and PVP K25 (Mw = 29,000 g/mol) were purchased from Sigma Aldrich (Dorset, UK) and used without further purification. PVP K12 (Mw = 2,500 g/mol) and Polyvinylpyrrolidone/vinyl acetate (PVP/VA64) (a ratio PVP to VA of 6:4; Mw = 45,000–70,000 g/mol, brand name Kollidon 64) were obtained from BASF Chemical Co. (Ludwigshafen, Germany) and used without further purification.

Methods

Sample Preparation

Ball milling was performed at room temperature using an oscillatory ball mill (Retsch, model MM200, Germany). In order to determine the extent of melting point depression of crystalline FD, mixtures containing drug weight fractions between 0 and 0.95 were prepared. One gram total mass of drug and polymer at various drug compositions were placed in a 25 mL milling chamber with a single, stainless steel ball ($\Phi = 15$ mm) and milled at 20Hz. Each milling cycle lasted two minutes followed by a cooling period of two minutes. This cycle was repeated until a total of eight minutes of milling had been completed. The milling time of eight minutes was found to be the point where no further reduction in the melting endotherm was obtained and the drug rendered partially amorphous. However, in the case of PVP K25, a milling time of sixteen minutes was required to optimize the particle surface interaction.

Thermal Analysis

Differential Scanning Calorimetry (DSC) experiments were performed using a TA Q100 (TA Instruments, United Kingdom) with nitrogen being selected as the purge gas. A previous study carried out by our group used a DSC heating rate of 1.0°C/min when determining the extent of melting point depression (11). The TA Q100 is capable of processing at this temperature as well as other lower heating rates (0.5°C/min and 5.0°C/min). Calibration deltaT of the instrument was carried out using high purity Indium at each specified heating rate. Standard TA aluminium pans were used with the lids being rested on the sample mixture. The mass of each sample in this study was maintained as close to 5.0 mg as possible throughout.

Effect of DSC Heating Rate

The excipients used in this study possess glass transition temperatures of 116°C (PVPK15) and 104°C (PVP/VA64). To examine the effect of heating rate upon the T_{end}, a series of DSC experiments were conducted whereby ball-milled samples were initially heated to 125°C (using a DSC heating rate of 50°C/min) and held isothermally for a period of five minutes. Subsequently, each sample was ramped to a temperature of 145°C using either a heating rate of 0.5, 1.0 or 5.0°C/min. At this temperature, drug melts and the characteristics (T_{end}, enthalpy) of the drug can be observed. Within this study, the end point of melting (T_{end}) was used to calculate the Flory Huggins interaction parameter (χ). The end point of melting was calculated from the intercept of the falling edge of melting endotherm with the post-melting baseline.

Time Above Polymer T_g

When examining the DSC programmes for each of the heating rates above, it can be observed that under these conditions each drug-polymer mixture will be subjected to varying times above the T_g of the polymer. Using a heating rate of 0.5°C/min, the drug-polymer mixture will be held at temperatures above the polymer T_g for a time of 45 min (isothermal time period of 5 min at a temperature of 125°C, 40 min of heating at 0.5°C/min and considering the time above polymer T_g when equilibrating at 125°C at 50°C/min as negligible). The 1.0°C/min programme resulted in a time above T_g of 25 min. This variation in time above the T_g of the parent polymer may subsequently affect the time that is provided for the dissolution of crystalline drug into polymer. In these experiments, the time above T_g was standardized to examine the effect on melting point depression and hence, the solubility and miscibility limits identified within the phase diagram. By increasing the isothermal time period at 125°C, the 1.0°C/min programme enabled drug-polymer mixing to take place for 45 min.

Effect of Polymer Molecular Weight (MW)

The effect of polymer molecular weight was examined by using three different molecular weight grades of PVP (K12, K15 and K25). A single DSC heating rate of 0.5°C/min was used across each FD-PVP system.

Detection of Drug-Polymer Glass Transition Temperature (T_g)

Following heating (0.5, 1.0 and 5.0°C/min) to 145°C, drug-polymer samples were rapidly cooled to 0°C at a rate of 50°C/min to produce amorphous solid dispersions. After an isothermal period of five minutes, the drug-polymer solid dispersions were then heated to 165°C using a DSC scanning rate of 5.0°C/min. This second heat cycle enabled the detection of the T_g for each solid dispersion. It should be noted that these heat-cool-heat cycles were performed until a constant T_g was obtained. Glass transition temperature was determined as the midpoint of heat flow signal.

Treatment of Data

In a recent publication, our research group has presented a methodology on how to construct thermodynamic drug-

polymer phase diagrams using melting point depression data (11). A brief summary of the approach will also be provided here. According to the Flory Huggins theory, the free energy of mixing for a drug-polymer system can be written as (14):

$$\Delta G = RT\left[\phi \ln\phi + \frac{1-\phi}{m}\ln(1-\phi) + \chi\,\phi\,(1-\phi)\right] \quad (1)$$

Where ΔG is the Gibb's free energy of mixing, R is the molar gas constant, T is the temperature (°K), ϕ is the volume fraction of the drug and m is ratio of the polymer volume to that of the lattice site. Also included in Eq. 1 is the Flory Huggins interaction parameter (χ). Negative values of χ give an indication of the presence of numerous adhesive bonds between the drug and polymer favouring miscibility, whereas positive interaction parameters describe drug-polymer systems with limited miscibility.

The use of melting point depression data to calculate the value of χ can be completed by the application of the following equation (15,16):

$$\left(\frac{1}{T_m} - \frac{1}{T_m^0}\right) = \frac{-R}{\Delta H_{fus}}\left[\ln\phi + \left(1-\frac{1}{m}\right)(1-\phi) + \chi(1-\phi)^2\right] \quad (2)$$

In the equation above, T_m and T_m^0 are the melting points of the pure drug within the polymeric matrix and the pure drug, respectively and ΔH_{fus} represents the heat of fusion of the pure drug (calculated by determining the area of the endothermic peak in the DSC scan. In our experiments this was carried out at each heating rate). To develop a phase diagram to accommodate variation in temperature, we need define the temperature dependence of the drug-polymer interaction parameter:

$$\chi = A + \frac{B}{T} \quad (3)$$

Through the application of this equation, a plot of χ vs. 1/T will enable calculation of the entropic (A) and enthalpic (B) contributions to χ. Once these constants have been determined, theoretically it is possible to calculate a value for χ at any melting temperature (14). This relationship has been utilized within this study since various drug-polymer mixtures with low drug content did not produce a clear endothermic peak when processed in the DSC.

The calculation of the position of the binodal curve can be determined through the application of Eq. 1. By constructing a plot of ΔG/RT versus ϕ, it is possible to observe how ΔG changes with varying composition at a certain temperature. It should be noted that these plots are constructed on the basis that χ is independent of ϕ (15). Inputting different χ values into Eq. 1 and applying the common tangent rule to the various ΔG/RT versus ϕ plots will enable construction of the binodal curve (22). Furthermore, the position of the spinodal curve can be calculated by determining the second derivative of the free energy of the drug-polymer system and equating to zero (22).

Prediction of Drug-polymer Miscibility Using Solubility Parameter Approach

In order to probe the compatibility of each drug-polymer system in this study, solubility parameters for FD, PVPK15 and PVP/VA64 were calculated using the van Krevelen group contribution method, which is defined as:

$$\delta_{total} = \sqrt{\delta_d^2 + \delta_p^2 + \delta_h^2} \quad (4)$$

Where δ_d and δ_p represent the components of dispersive and polar forces and δ_h quantifies the total hydrogen bond energy of a particular component. Each of these elements can be calculated as follows:

$$\delta_d = \frac{\sum F_{di}}{V}; \delta_p = \frac{\sum F_{pi}^2}{V}; \delta_h = \sqrt{\frac{\sum E_{hi}}{V}} \quad (5)$$

Where F_{di} is the group contribution to dispersive forces, F_{pi} is the polar group component, E_{hi} represents the group contribution to hydrogen bond energy and V signifies the calculated molar volume of the component (23). If the difference in solubility parameters of a potential drug-polymer system exists within 7 $MPa^{1/2}$ the attainment of miscibility is a distinct possibility (11,24).

In addition to the application of melting point depression data to calculate the value of χ, solubility parameters can also be utilized to determine the level of interaction in a drug-polymer system by use of the following equation (22):

$$\chi = \frac{V_0}{RT}\left(\delta_{drug} - \delta_{poly}\right)^2 \quad (6)$$

where V_0 is the volume of the lattice site. The molar volumes of PVPK15 and PVP/VA64 were inputted into Eq. 6 in order to calculate χ values for both drug-polymer systems.

RESULTS AND DISCUSSION

Melting Point Depression and Gibb's Free Energy Plot

The objective of the eight-minute milling cycle adopted in this study was to maximize drug-polymer surface interactions. However, the preparation of physical mixtures in this way may also render the drug partially amorphous. Both of these milling effects contribute to the reduction of the chemical

potential of the drug (11), however, a further reduction of the melting point may be observed through the increasing fraction of polymer. A reduction in chemical potential can then be validated through the detection of melting point depression, most commonly observed using DSC (16,25). The alteration of the melting point of the drug compound will be dependent upon the type of mixing that ensues i.e. exothermic, endothermic or athermal. Exothermic mixing results in melting point depression. If a system is immiscible, melting point depression will not occur (15).

Figure 1a and b represent melting endotherms produced for FD-PVPK15 and FD-PVP/VA64 mixtures with a DSC heating rate of 0.5°C/min. It is evident that melting point depression occurs within each drug-polymer system. For example, the addition of 15% and 30% by weight of PVPK15 to FD reduces T_{end} from 141.09°C to 137.83°C and 129.67°C, respectively. Moreover, within the PVP/VA64 system, the addition of similar quantities of polymer (15 and 30% w/w PVP/VA64) significantly reduces T_{end} from 141.09°C to 139.70°C and 136.73°C, respectively. As previously discussed, drug-polymer miscibility is an essential prerequisite to the formulation of molecular dispersions and through the use of melting depression one can begin to gather information on the likelihood of mixing between two components. These results suggest drug-polymer miscibility at a temperature close to the melting point of the crystalline drug. Although such information is useful, there is no understanding of how miscibility changes as a function of drug load and/or temperature without further processing of thermal data (11). Through the use of Flory-Huggins theory, it is possible to use these data to evaluate polymeric candidates for suitability in formulation of solid dispersions using limited quantities of drug substance (26).

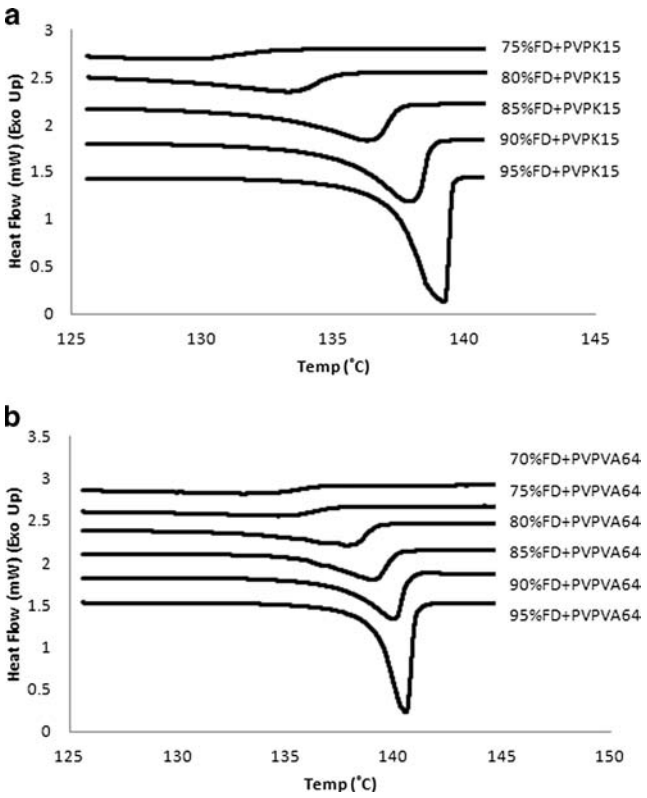

Fig. 1 **(a)** DSC thermograms of ball-milled FD-PVPK15 mixtures obtained using a DSC heating rate of 0.5°C/min with various drug loadings of FD, (**b**) DSC thermograms of ball-milled FD-PVP/VA64 mixtures obtained using a DSC heating rate of 0.5°C/min with various drug loadings of FD.

To better understand miscibility between two components, consideration of the temperature effect on Gibb's free energy is useful. In drug-polymer combinations exhibiting a negative ΔG at defined temperature, miscibility is thermodynamically favoured (27,28). Drug-polymer miscibility, at temperatures close to the melting point of the drug, can be examined through the application of Eq. 1. Using this single point χ (15), a plot of $\Delta G/RT$ versus φ can be created.

Melting point depression data was determined for each system using a DSC heating rate of 0.5°C/min. These T_{end} values were then used to construct a plot of χ versus 1/T for each drug-polymer system which enabled the calculation of the entropic (A) and enthalpic (B) contributions to χ for FD-PVPK15 and FD-PVP/VA64 (see Table I). These values were inputted into Eq. 3 to calculate χ for each system at an elevated temperature, where it may be a reasonable to assume that a certain degree of drug-polymer miscibility will be obtained, in this case, a temperature of 100°C was selected. For FD-PVPK15, the value of χ was −0.53, indicating an exothermic heat of mixing and the attainment of miscibility between FD and PVPK15 (11). However, for FD-PVP/VA64, the associated χ value at 100°C was 3.18. The positive nature of χ indicates that FD-PVP/VA64 will not be miscible at this elevated temperature. Using these χ values for each drug-polymer system, a Gibb's free energy plot, as described above, was plotted and the results can be observed in Fig. 2. Through the construction of these plots, we can start to fully understand the variation in Gibb's free energy as a function of both temperature and composition.

Table I Calculated Entropic and Enthalpic Constants Determined Through Linear Regression Analysis of Melting Point Depression Data for FD-PVPK15 and FD-PVP/VA64 Using 0.5°C/min Heating Rate and χ Values Calculated at a Temperature of 25°C. Difference in Solubility Parameters of Each Drug-polymer System Using Van Krevelen Group Contribution Method

	FD-PVPK15	FD-PVP/VA64
A	−13.889	−33.553
B	4984.4	13699.7
$\Delta\delta$ $(MPa)^{1/2}$	2.97 (24.393-21.417)	5.593 (24.393-18.80)
χ^a	2.837	12.419
χ^b	0.125	0.584

[a] Determined through the extrapolation of melting point depression data to 25°C. [b] Calculated using van Krevelen solubility parameter method at 25°C.

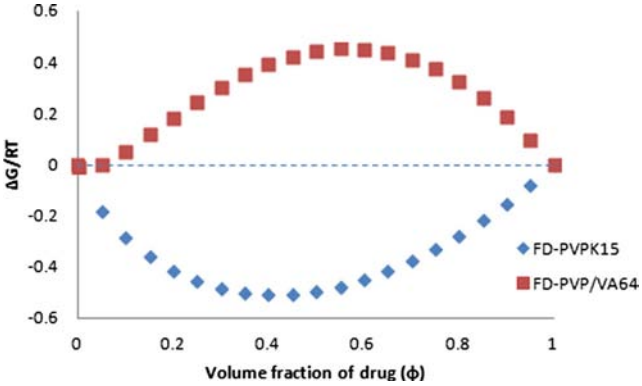

Fig. 2 A plot of ΔG/RT versus drug volume fraction (φ) for FD-PVPK15 and FD-PVP/VA64 with respective χ values calculated at 100°C (using a DSC heating rate of 0.5°C/min).

It is apparent from the negative Gibb's free energy of mixing across all possible drug loads that FD will form a miscible system with PVPK15 at 100°C. However, based on the positive Gibb's free energy produced between FD and PVP/VA64 across volume fractions≥0.05, it can be predicted that miscibility is not favourable with this particular drug-polymer system at 100°C. Interestingly, using PVPK15, the Gibb's free energy is negative at temperatures of 80°C and higher, across pharmaceutical relevant drug weight fractions (≤0.99). However, at temperatures of 50°C and 25°C there are drug weight fractions≥0.43 and≥0.08, respectively, that result in positive Gibb's free energy values. In such cases, this would suggest immiscibility. By way of comparison to PVPK15, PVP/VA64 exhibits positive Gibb's free energy values at temperatures of 120°C and lower. At this temperature for PVP/VA64, drug fractions≥0.58 result in positive Gibb's free energy values. This information is particularly useful in not only selecting the most appropriate polymer for formulation purposes but may also help guide selection of processing temperature during hot melt extrusion in order to maximize drug-polymer miscibility.

Solubility Parameter Evaluation

One approach to determine the compatibility of drug-polymer combinations that has been used extensively in the literature is the application of solubility parameter calculations. Within this study, the van Krevelen group contribution method was applied to FD, PVPK15 and PVP/VA64 and these values are shown in Table I. Both drug-excipient systems possess Δδ values of less than 7 $MPa^{1/2}$ suggesting that miscibility will be obtained in each case (24). However, the proximity of the solubility parameters of FD-PVPK15 is more favourable than the value produced between FD-PVP/VA64. This data would suggest that a higher degree of miscibility is produced between FD-PVPK15 when compared to FD-PVP/VA64. Furthermore, calculation of a single χ value for each system through the application of Eq. 6 demonstrated the greater compatibility between FD-PVPK15. Although both χ values are positive when using this approach for polymer screening, possible inaccuracies in the methodology have previously been cited, including the potential inability of this equation to adequately describe polar systems (16,22,29).

Effect of DSC Heating Rate

In recent literature discussing the application of the FH theory to melting point depression data, DSC heating rates ranging from 0.2°C/min (18) - 10°C/min (21) have been utilized. When increasing DSC heating rate, the temperature differential produced between the sample and reference pans is increased and will result in a larger value of T_{end} being elucidated (30). Fig. 3 shows plots of sample temperature versus time for 95% FD-PVPK15 with the three DSC heating rates employed in this study. It should be noted that larger thermal lags were detected for FD-PVP/VA64 at the same DSC heating rate. Therefore, from our understanding, additional effects other than DSC heating rate are present in these drug-polymer systems that are also driving the observed changes in T_{end}. The effects of drug-polymer interaction and polymer thermal conductivity (and in-turn, mixture viscosity) will also play a role in determining the extent of melting point depression for a drug-polymer system. Information documenting the effects of DSC heating rate on the extent of drug-polymer interaction and viscosity is limited at this time. A slower DSC heating rate will give rise to increased time above the T_g of the parent polymer. This could potentially increase drug-polymer interaction as more time is given for dissolution of the drug into rubbery polymer. The implications of these heating effects will be discussed further in the construction of thermodynamic drug polymer phase diagrams.

In the comparison of excipient selection previously discussed, melting point depression data was collected using a DSC heating rate of 0.5°C/min. Application of the calculated entropic and enthalpic constants (Table I) to an elevated temperature of 120°C produces a χ value of −1.21 when Eq. 3 is employed. This negative value indicates an exothermic heat of mixing and the attainment of miscibility between FD and PVPK15 (11). The prediction of miscibility under these conditions is further validated by the negative Gibb's free energy of mixing obtained across all drug volume fractions in Fig. 4.

When detecting the endpoint of melting using a DSC heating rate of 1.0°C/min, significant changes in the entropic and enthalpic contributions to χ were observed (A=−61.31 and B=24476.20). Calculation of χ at a temperature of 120°C using these constants yielded a value of 0.97. The

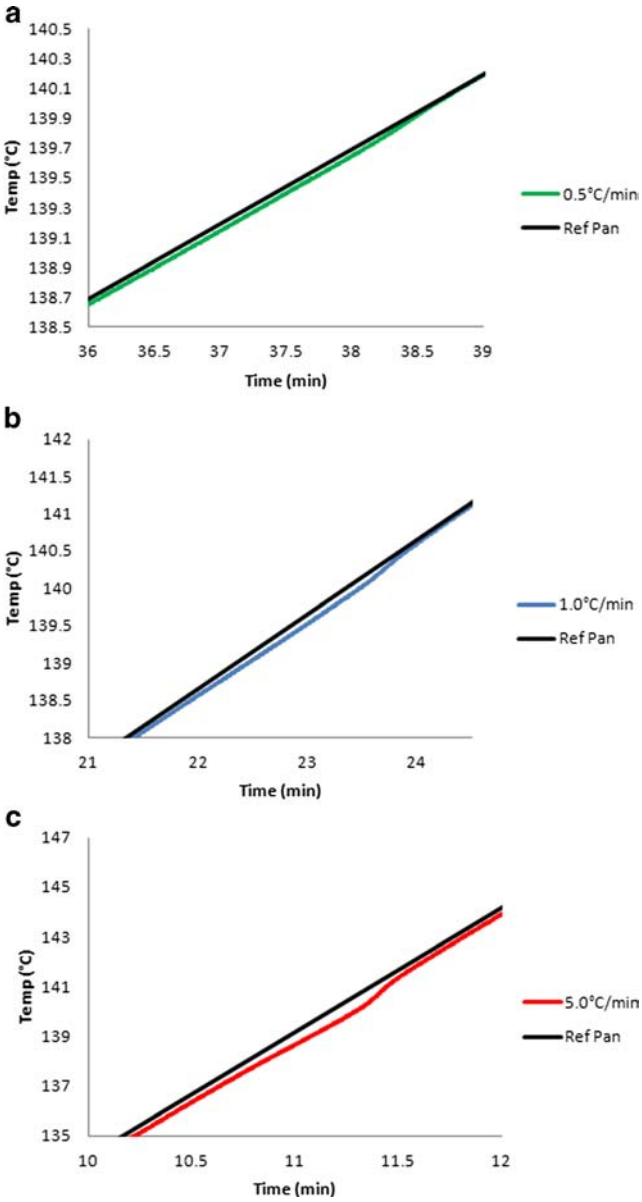

Fig. 3 Temperature differential produced between reference and sample pans containing 95%FD-PVPK15 when heating rates of 0.5°C/min (**a**), 1.0°C/min (**b**) and 5.0°C/min (**c**) are applied.

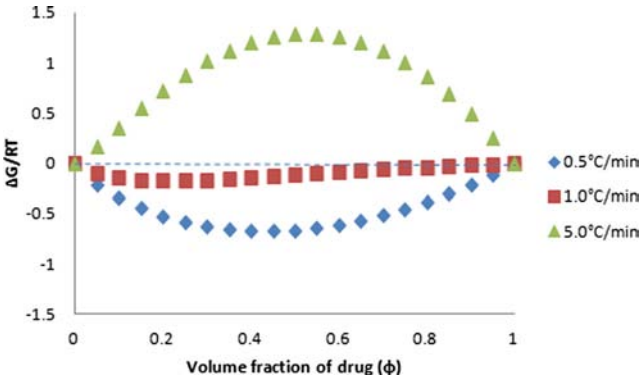

Fig. 4 A plot of ΔG/RT versus drug volume fraction (φ) for FD and PVPK15 with respective χ values calculated at 120°C using 0.5, 1.0 and 5.0°C/min DSC heating rate.

positive nature of χ indicates the less favourable nature of mixing between FD and PVPK15 when employing a heating rate of 1.0°C/min. However, the attainment of a negative Gibb's free energy across all drug loadings signifies FD-PVPK15 miscibility due to favourable entropic contributions to mixing present in this drug-polymer system at 120°C (15).

Similarly, melting point depression data produced with a DSC heating rate of 5.0°C/min led to the calculation of a positive χ value (6.59) at 120°C when using A and B values of −241.92 and 97666.88 respectively. Fig. 4 displays how; in this case, the Gibb's free energy of mixing is positive across≥ 0.999 drug volume fraction. It is clear from this figure that changes in the calculated values of A and B will significantly impact upon the Gibb's free energy of mixing for a particular drug-polymer system at a certain temperature.

Effect of Polymer Molecular Weight

We acknowledge that, when changing the molecular weight of PVP, the viscosity will be different and we also assume there is no difference in drug-polymer interaction (31). Hence we may be able to probe the effect of viscosity in the construction of FH phase diagram. In this experiment, three molecular weights of PVP (K12, K15 and K25) were used. DSC measurement of a sample containing 15% w/w PVPK12 with FD resulted in a reduction of T_{end} from 141.09°C (pure FD) to 136.43°C whereas the addition of the same amount of PVPK25 produced a T_{end} value of 138.01°C. By reducing the molecular weight of the polymer, the dissolution of the drug into the polymer matrix is not inhibited by the effects of polymeric viscosity. Marsac and co-workers found that the solubility of FD decreases with increasing polymer MW until a critical point is reached. These effects were rationalized by considering the term, (1 − 1/m) approaches 1 as the MW of the polymer is increased (15) (see Eq. 2).

We recognize that the T_g of PVPK25 is higher than the melting point of FD and the application of Eq. 2 to this drug-polymer system may not be appropriate (15). However, due to the attainment of melting point depression, most likely caused by the process of ball milling (11,25), the calculation of a range of χ values was made possible.

The differences in T_{end} data when the molecular weight of the excipient is varied will also impact upon the calculated entropic and enthalpic contributions to the Gibb's free energy of mixing. As can be seen through the application of Eq. 1, across all drug weight fractions, the entropic contribution to the Gibb's free energy of mixing was more favourable for the lower MW PVP, which results in a value of m closer to 1. The ratio of the molar volume of the PVPK12 polymer chain to

that of the FD lattice site is lower than the calculated values for FD-PVPK15 and FD-PVPK25.

Phase Diagram Construction

Comparison of Polymer Type

A drug-polymer phase diagram constructed by applying the Flory Huggins theory to melting point depression data from a thermal analysis method, such as DSC, will most likely produce an underestimation of the amorphous drug miscibility that could be achieved though hot-melt extrusion processing. Within a hot melt extruder, the screws will impart shear stresses on the drug-polymer mixture and will most likely produce a system with improved homogeneity in comparison to a ball milled sample that is processed in the DSC, especially with polymeric excipients with high viscosities. Therefore, great care needs to be taken when designing the appropriate DSC programme for a drug-polymer system to enable the prediction of certain process conditions.

Using the melting point depression data obtained with a DSC heating rate of 0.5°C/min; thermodynamic drug-polymer phase diagrams were constructed for FD-PVPK15 and FD-PVP/VA64, which enabled a comparison of the selection of polymer type (see Fig. 5). For the classic Flory-Huggins theory consisting of binodal and spinodal curves, Upper Critical Solution Temperature (UCST) behaviour has been obtained in all of our drug-polymer systems. This type of behaviour arises when the calculated value of B (Eq. 3) is greater than zero. In other words, the value of the interaction parameter decreases with increasing temperature (22). It should also be noted that the liquid–solid line for each drug-polymer system exists entirely above each set of FH curves. If we analyse of the position of each spinodal curve in Fig. 5 and consider 25°C as a relevant pharmaceutical storage temperature, it can be observed that PVPK15 can remain within a metastable region with a significantly larger weight fraction of FD than PVP/VA64. The area beneath the spinodal curve is unstable to any small fluctuation in drug density and should such a fluctuation occur, spontaneous phase separation, also known as spinodal decomposition will take place.

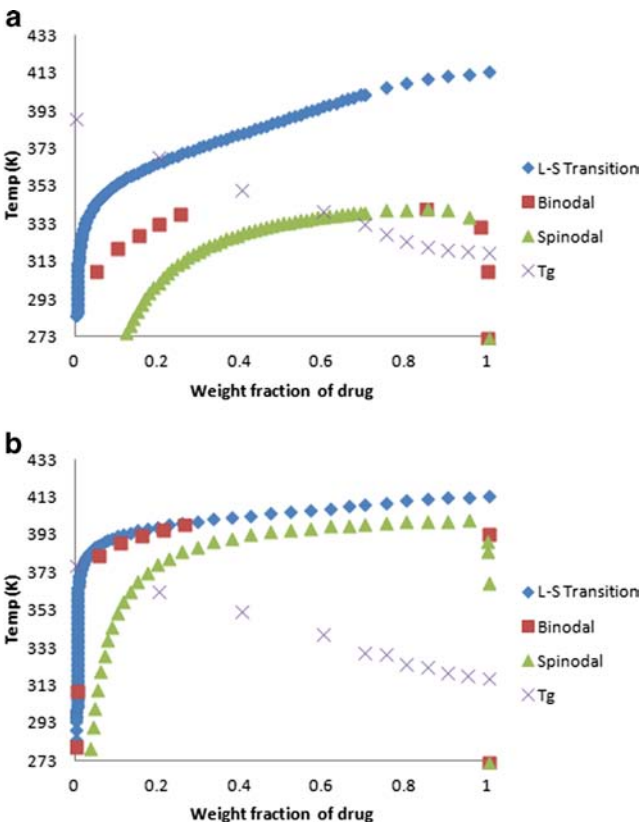

Fig. 5 A comparison of the completed phase diagrams of FD-PVPK15 (**a**) and FD-PVP/VA64 (**b**) constructed with melting point depression data determined at 0.5°C/min.

Within the metastable zone, although the phase-separated state may be thermodynamically favourable, the drug-polymer system will be stable to small fluctuations in drug density (11,22). Large fluctuations in drug density will initiate drug polymer phase separation via a nucleation and growth mechanism, whereby drug molecules within the solid dispersion first phase separate from the mixture and then form as droplets and to grow in size (11,14,22). However, if such system can be stored below their T_g, the physical stability may be further enhanced by the dramatic increases in the viscosity of the system (10 fold increase as temperature drops below the T_g (13)). For example, if the drug-polymer mixture is stored at a temperature sufficiently beneath the T_g of the system, a reduction in molecular mobility will ensue and phase separation may be significantly inhibited (6,11,32).

Other than straightforward data processing for the spinodal curve of the phase diagram, we also tried to probe the mathematic calculation of binodal curve in our study. Fig. 6 demonstrates how the binodal curves were constructed for each drug-polymer system. The common tangent rule identifies the two drug loadings that possess the lowest Gibb's free energy across all drug compositions at a particular temperature. Within the pair of drug loading values calculated following this method, one point will exist at a lower drug loading than the UCST and the other will exceed this critical value. The common tangent rule can be applied with practical results for certain drug loadings (w/w less than 0.3 and bigger than w/w of UCST). Mathematic results for these points in the middle do exist but there is no practical meaning; in another words, the intercept point results in a temperature value above the critical temperature of UCST due to asymmetric plot of free energy curve of the drug-polymer system (33). For each drug-polymer phase diagram, the common tangent rule could only identify binodal curve positions at drug weight fractions <0.30 and $>$ UCST. This resulted in the identification of an undefined region between ~0.30 and UCST weight fractions for both drug-polymer systems. In

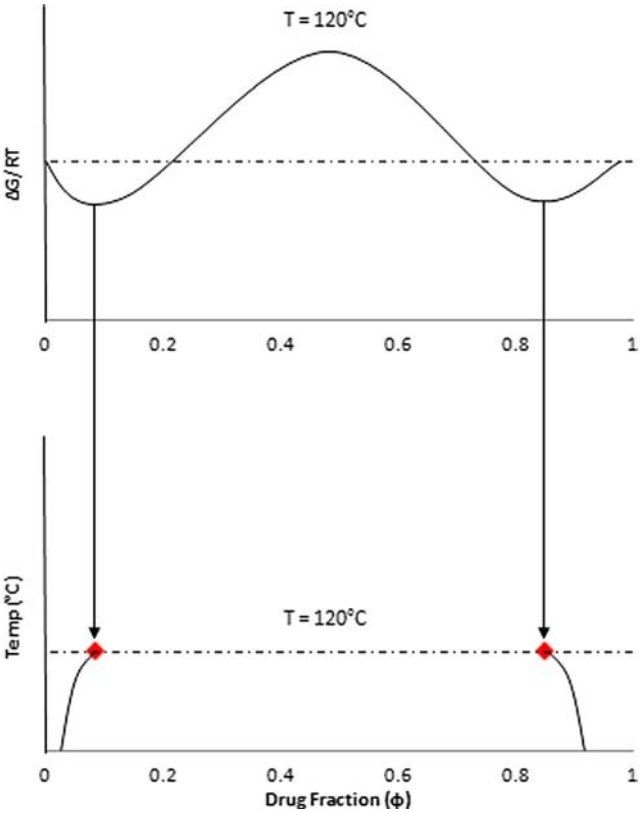

Fig. 6 Application of the common tangent rule in binodal construction for a drug-polymer system.

order to overcome this limitation in the binodal construction for this small drug molecule-polymer system, critical ϕ and χ values were calculated for FD-PVPK15 and FD-PVP/VA64 (22). The weight fraction and temperature values that were identified specified the critical limits whereby the common tangent rule could still be applied for each drug-polymer system.

Effect of DSC Heating Rate

As construction of the drug-polymer phase diagram is hugely dependent upon the T_{end} and the linear relationship between calculated χ values and 1/T, the selection of DSC heating rate will undoubtedly have a significant impact on the relative position of the calculated solubility and miscibility curves constructed using a Flory Huggins model. It should also be noted that the selection of the onset, endpoint or maximum peak of the melting endotherm is another point that must be considered when collecting melting point depression data. The rationale for selecting the end point of melting in this study is because it represents the temperature of the homogenous liquid state of the drug-polymer system. Such an assumption has been verified in all our phase diagram data that the liquid solid line sits above all binodal and spinodal curve (15).

Different DSC heating rate gave us various drug-polymer miscibility limits (i.e. spinodal intercept on drug loading at defined temperature). Lower heating rates resulted in an increased miscibility limit in which the spinodal curve produced using a DSC heating rate of 0.5°C/min produced the greatest miscibility limit ($P<0.05$). The discrepancies in spinodal curve positions identified in FD-PVPK15 drug-polymer phase diagrams in Fig. 7 can be attributed to the calculation of the entropic and enthalpic contributions to χ when using different DSC heating rates to characterize melting point depression. As heating rate is increased from 0.5°C/min to 5.0°C/min, the value of A changes from −13.889 to −241.93 and B increases from 4984.4 to 97666. When these values are inputted into the second derivative of Eq. 1, it is clear from Fig. 7 that the position of the spinodal curve is significantly affected. The largest miscibility limit of drug in the polymer system that produced by the spinodal curve could have significant implications when applied to a processing technique such as HME. The liquid–solid transition curve identifies the optimum extrusion conditions for a particular drug-polymer system (34). When the extrudate is cooled to pharmaceutically relevant storage temperatures the miscibility, or spinodal curve, can be used as a guideline to predict at what drug loading the amorphous solid dispersion will be stable to small fluctuations in density. Hence a critical determination of an appropriate DSC method would have significant impact upon the understanding of physical stability of drug polymer binary solid dispersion system.

The broadening of the melt and apparent increase in T_{end} when applying increased DSC heating rates is one of the main reasons driving the changes in melting point depression data and calculation of A and B. However, as previously discussed, it is necessary to consider the effects that heating rate has on the extent of drug-polymer interaction and the viscosity of the drug-polymer mixture. It is generally accepted that slow DSC heating rates enable molecules from within a crystal lattice to dissolve within a polymeric excipient more readily than higher

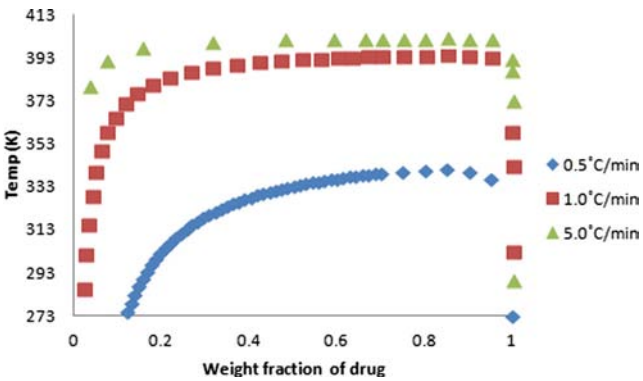

Fig. 7 A comparison of the various calculated spinodal curve positions produced for FD-PVPK15 when DSC heating rates of 0.5, 1.0 and 5.0°C/min are applied.

heating rates (35,36). One potential technique to minimize the effects of the temperature differential, or lag, produced between reference and sample pans when various heating rates are implemented could be the extrapolation to a theoretical zero heating rate (30). Extrapolation of melting point depression data to a theoretical 0°C/min DSC heating rate when detecting the solubility of a crystalline drug within a polymeric matrix has previously been examined (25,37,38). An extrapolation to this theoretical heating rate was attempted within this study for the FD-PVPK15 system. However, it was apparent that a linear regression could not be constructed with sufficient reliability to enable an extrapolation. In the literature, where this technique has been utilized previously, heating rates between 0.1 and 1.0°C/min enabled a much higher linear regression to be constructed with the melting point depression data when a weak dependence on the heating rate was observed. It may be attributed to the fact that, weak interactions were obtained between these two components, e.g. D-mannitol in PVPK15 (25) and our system of FD in PVP/VA64 (where a much higher linear regression was achieved compared to FD-PVPK15). Furthermore, an appropriate mixing technique may also have huge influence on the homogeneity of the physical mixture, where a significant heating rate dependence may be observed from a less homogenized physical mixture. With improved drug-polymer mixing before analysis in the DSC, drug particles will require less diffusion to achieve a liquid-liquid equilibrium state (25). Similar effects were observed for increasing DSC heating rate when applied to the FD-PVP/VA64 system. Statistically significant differences were detected between the miscibility limits produced using melting point depression data from DSC heating rates of 0.5, 1.0 and 5.0°C/min ($P<0.05$). Therefore, the phase diagrams of FD-PVPK15 and FD-PVPVA were both calculated using the lowest heating rate (Fig. 5).

Drug-polymer Time Above Parent Polymer T_g

The polymeric excipients PVPK15 and PVP/VA64 possess different T_g values, therefore FD-PVPK15 and FD-PVP/VA64 samples were equilibrated at 125°C for 5 min so each polymer would act as a viscous solvent from the beginning of the thermal analysis. By ramping at various heating rates after this isothermal time period had elapsed, the drug-polymer mixing time above the parent polymer T_g has varied. In our study, we have adjusted the annealing time at temperature 125°C for heating rate 1°C/min to achieve the same total experiment time above T_g of the polymer as used with the 0.5°C/min heating rate. Fig. 8a displays a summary of the various DSC programmes that have been implemented in this study for FD-PVPK15 at different heating rates. The positions of the spinodal curves constructed for FD-PVPK15 using the original melting point depression data at 1°C/min (programme 2) and the values obtained when standardising the

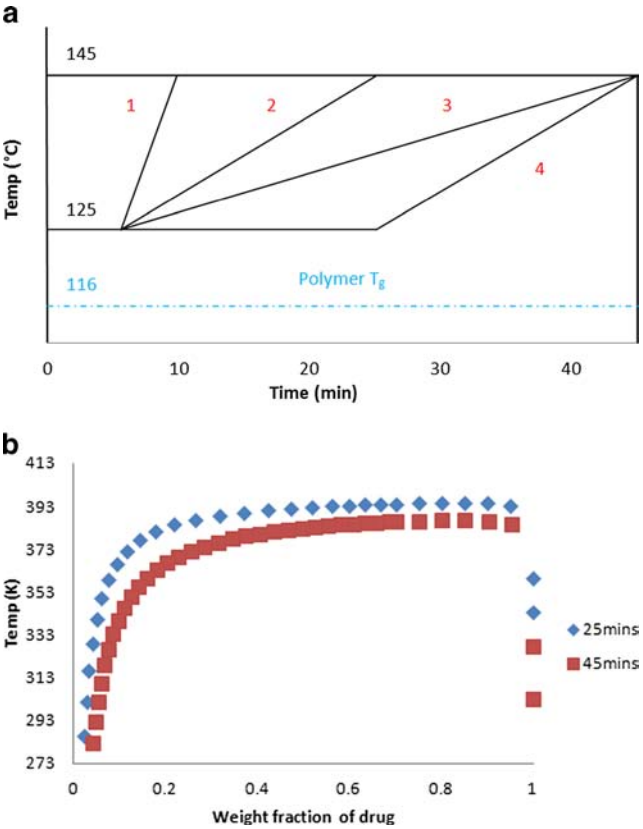

Fig. 8 (**a**) Schematic demonstrating the four DSC programmes adopted when studying melting point depression in changes in FD-PVPK15, (**b**) Calculated spinodal curve positions produced when the time above polymer T_g is varied for FD-PVPK15 at 1°C/min.

drug-polymer time above the polymer T_g (programme 4) are shown in Fig. 8b. It was determined that increasing the time period whereby the polymer acts as a viscous solvent produced an improvement in the miscibility limit identified by the spinodal curve at a temperature of 25°C and other relevant pharmaceutical storage temperatures (see Table II). This finding holds particular significance in phase diagram construction as it demonstrates the potential in increasing drug-polymer interaction when this time period above the polymer T_g is extended. It may also be the case that increasing time above polymer T_g reduces the ability of polymer viscosity to inhibit the dissolution of the drug into rubbery polymer. In other words, increasing the experiment time above the parent polymer T_g would significantly improve diffusive mixing during the DSC measurement (25), hence providing more accurate date for the construction of drug-polymer phase diagrams.

Effect of Polymer Molecular Weight (MW)

The solubility of FD in varying molecular weight grades of PVP has previously been examined through the use of melting point depression data and calculation of the activity coefficient of the drug within the polymeric excipient (15). However, the

Table II Binodal and Spinodal Curve Positions at Three Relevant Pharmaceutical Storage Temperatures (4, 25 and 40°C). a = 0.5°C/min DSC Heating Rate, b = 1.0°C/min, c = 1.0°C/min with 45 min Above Polymer T_g and d = 5.0°C/min

	Drug Weight Fraction					
	Binodal Curve Position			Spinodal Curve Position		
Temperature (°C):	4	25	40	4	25	40
System						
PVPK12[a]	1.92E-2	7.21E-2	1.74E-1	1.61E-1	2.56E-1	4.14E-1
PVPK15[a]	6.68E-3	2.63E-2	6.58E-2	1.24E-1	1.80E-1	2.52E-1
PVPK25[a]	3.43E-4	2.28E-3	6.10E-3	7.24E-2	9.89E-2	1.29E-1
PVP/VA64[a]	5.00E-8	1.60E-6	1.45E-5	3.35E-2	4.28E-2	5.21E-2
PVPK15[b]	1.88E-13	3.49E-10	1.78E-8	1.88E-2	2.44E-2	3.01E-2
PVPK15[c]	1.56E-7	8.48E-6	6.86E-5	3.62E-2	4.74E-2	5.88E-2
PVPK15[d]	1.8E-51	2.15E-38	1.37E-31	4.59E-3	5.92E-2	7.25E-3

application of melting point depression data of FD with varying PVP molecular weight grades to construct temperature dependent drug-polymer phase diagrams is yet to be examined. The resulting drug-polymer phase diagrams for each drug-PVP (K12, K15 and K25) system of varying molecular weight shows that PVPK12 produces the largest miscibility limit (Fig. 9), verified by statistical analysis ($P<0.05$). Table II provides data regarding the positions of the binodal and spinodal curves when using different MW grades of PVP. It was determined that PVPK12 produced the greatest miscibility limit across all three relevant pharmaceutical storage temperatures. We hypothesize that by incorporating a low molecular weight PVP grade, the viscosity and free volume of the polymer will promote dissolution of FD and hence the extent of melting point depression is greater and the calculation of A and B produce more favourable values in comparison to PVPK15 and PVPK25.

Concept and Implication of Phase Diagram

Thermodynamically, any system under the liquid–solid is a non-equilibrium system and should undergo a recrystallization process. However, kinetically the binodal and spinodal curves can be defined. The dynamic of recrystallization of amorphous drug from the mixture should be highly controlled by these non-equilibrium phenomena, i.e. the phase separation and recrystallization.

A typical FH theory-based phase diagram is normally used to describe the behaviour of liquid-liquid mixture, in which a binodal curve, separating the one-phase liquid-liquid mixture and coexisting two-phase metastable mixture; and a spinodal curve, which separates the metastable liquid-liquid mixture and spontaneously unstable mixture. The defined temperature at which these two curves meet is called the upper or lower critical solution temperature (UCST or LCST) depending on the shape of the binodal and spinodal curves (Fig. 10).

Thermodynamic phase diagrams and phase separation dynamics have been widely studied for the binary systems of two amorphous polymers, semicrystalline polymer - amorphous polymer and two semicrystalline polymers (39,40). In any mixture involving semicrystalline polymer there is an opportunity for the mixture to display a composition-dependent melting point. For example in Fig. 10, where a typical UCST phase diagram was presented, the melting point curve (liquid–solid line) can be either entirely above

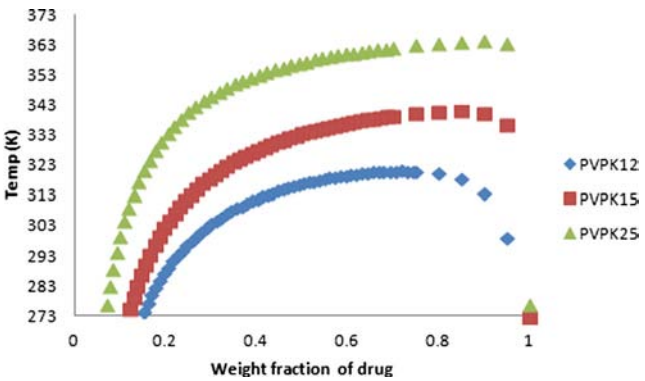

Fig. 9 Calculated spinodal curve positions of FD-PVP systems containing different molecular weights of PVP

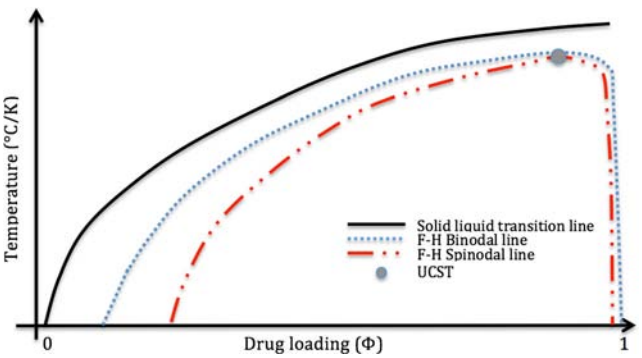

Fig. 10 The phase diagram constructed using Flory-Huggins liquid-liquid mixing system and liquid–solid dissolution system. The typical position of the liquid–solid line in the Flory-Huggins system where it exists above all FH theoretical curves

the FH curves or cross through the FH curves. The liquid–solid (melting point of the mixture) curve is dependent on the compositions of the amorphous polymeric carrier and normally a melting depression is observed from the mixture. Thermodynamically the FH phase diagram can only be used to describe the system when both components are liquid i.e. above the liquid–solid line, and the melting point curve cannot be identified below the binodal curve. The position of the liquid–solid line in FH phase diagram will significantly affect the dynamic of crystallization.

In all drug-polymer systems that have been studied from our group, the position of liquid–solid curve always sits above the FH curves, which means the drug will always crystallize at any temperature below the liquid–solid line. However such crystallization is drug composition dependent. We have observed that, when the drug loading is higher than a critical value (e.g. 0.5-0.6 w/w in FD/PVP at temperature 80°C), the crystallization of small molecule from the solid dispersion is a solid–liquid phase separation; in contrast, for a sample containing less drug, a liquid-liquid phase separation is the precursor to crystallization. In other words, the principle of phase separation that can be defined by the FH theory may be successfully implicated in our system when the drug loading is less than a certain critical value. The construction of the FH diagram together with the liquid–solid line have provided us with a further understanding of the stability of amorphous drug and polymer solid dispersion system.

CONCLUSION

In this study, thermodynamic drug-polymer phase diagrams have been created by applying the FH theory to the melting point depression data of two drug-polymer systems. The current understanding of drug-polymer phase diagrams is also reviewed. The comparison of the miscibility limits of each drug-polymer system demonstrated that PVPK15 was able to incorporate comparable greater weight fraction of FD when compared to PVP/VA64. The effects of the DSC heating rate applied to detect melting point depression data on the construction of a drug-polymer phase diagram have been discussed for the first time. It was apparent that the use of lower DSC heating rates identified a potentially larger metastable region at pharmaceutically relevant storage temperatures. However, the improvement in miscibility limit cannot be attributed to DSC heating rate alone, the effects of drug-polymer interaction and polymer thermal conductivity will also play a role in the thermal analysis techniques employed. The effects of drug-polymer annealing time above polymer T_g have also been investigated. It was observed that increasing the time above parent polymer T_g resulted in an enhancement in the calculated miscibility limits at various pharmaceutically relevant storage temperatures. PVPK12 produced an enhancement in the miscibility limit when compared to K15 and K25 MW grades. The relevance of these findings when applied to a processing method such as HME has also been discussed.

REFERENCES

1. Ku MS, Dulin W. A biopharmaceutical classification-based Right-First-Time formulation approach to reduce human pharmacokinetic variability and project cycle time from First-In-Human to clinical Proof-Of-Concept. Pharm Dev Technol. 2012;17:285–302.
2. Andrews GP, Abu-Diak O, Kusmanto F, Hornsby P, Hui Z, Jones DS. Physicochemical characterization and drug-release properties of celecoxib hot-melt extruded glass solutions. J Pharm Pharmacol. 2010;62:1580–90.
3. Merisko-Liversidge EM, Liversidge GG. Drug Nanoparticles: Formulating Poorly Water-Soluble Compounds. Toxicol Pathol. 2008;36:43–8.
4. Kawabata Y, Wada K, Nakatani M, Yamada S, Onoue S. Formulation design for poorly water-soluble drugs based on biopharmaceutics classification system: basic approaches and practical applications. Int J Pharm. 2011;420:1–10.
5. Huang L, Tong W. Impact of solid state properties on developability assessment of drug candidates. Adv Drug Deliv Rev. 2004;56:321–34.
6. Hancock B, Zografi G. Characteristics and significance of the amorphous state in pharmaceutical systems. J Pharm Sci. 1997;86:1–12.
7. Leuner C, Dressman J. Improving drug solubility for oral delivery using solid dispersions. Eur J Pharm Biopharm. 2000;50:47–60.
8. Alam MA, Al-Jenoobi FI, Al-mohizea AM. Commercially bioavailable proprietary technologies and their marketed products. Drug Discov Today. 2013;18:936–49.
9. Lewis S, Dhirendra K, Udupa N, Atin K. Solid dispersions: a review. J Pharm Sci. 2009;22:234.
10. Laitinen R, Lobmann K, Strachan CJ, Grohganz H, Rades T. Emerging trends in the stabilization of amorphous drugs. Int J Pharm. 2013;453:65–79.
11. Tian Y, Booth J, Meehan E, Jones DS, Li S, Andrews GP. Construction of Drug-Polymer Thermodynamic Phase Diagrams Using Flory-Huggins Interaction Theory: identifying the Relevance of Temperature and Drug Weight Fraction to Phase Separation within Solid Dispersions. Mol Pharm. 2013;10:236–48.
12. Mahieu A, Willart J, Dudognon E, Danede F, Descamps M. A New Protocol To Determine the Solubility of Drugs into Polymer Matrixes. Mol Pharm. 2013;10:560–6.
13. Friesen DT, Shanker R, Crew M, Smithey DT, Curatolo WJ, Nightingale JAS. Hydroxypropyl Methylcellulose Acetate Succinate-Based Spray-Dried Dispersions: an Overview. Mol Pharm. 2008;5:1003–19.
14. Lin D, Huang Y. A thermal analysis method to predict the complete phase diagram of drug-polymer solid dispersions. Int J Pharm. 2010;399:109–15.
15. Marsac PJ, Li T, Taylor LS. Estimation of Drug-Polymer Miscibility and Solubility in Amorphous Solid Dispersions Using Experimentally Determined Interaction Parameters. Pharm Res. 2009;26:139–51.
16. Marsac PJ, Shamblin SL, Taylor LS. Theoretical and practical approaches for prediction of drug-polymer miscibility and solubility. Pharm Res. 2006;23:2417–26.
17. Albers J, Matthee K, Knop K, Kleinebudde P. Evaluation of Predictive Models for Stable Solid Solution Formation. J Pharm Sci. 2011;100:667–80.

18. Zhao Y, Inbar P, Chokshi HP, Malick AW, Choi DS. Prediction of the Thermal Phase Diagram of Amorphous Solid Dispersions by Flory-Huggins Theory. J Pharm Sci. 2011;100:3196–207.
19. Caron V, Tajber L, Corrigan OI, Healy AM. A Comparison of Spray Drying and Milling in the Production of Amorphous Dispersions of Sulfathiazole/Polyvinylpyrrolidone and Sulfadimidine/Polyvinylpyrrolidone. Mol Pharm. 2011;8:532–42.
20. Tian Y, Caron V, Jones DS, Healy A, Andrews GP, Tian Y, *et al.* Using Flory–Huggins phase diagrams as a pre-formulation tool for the production of amorphous solid dispersions: a comparison between hot-melt extrusion and spray drying. J Pharm Pharmacol. 2014;66:256.
21. Yang M, Wang P, Gogos C. Prediction of acetaminophen's solubility in poly(ethylene oxide) at room temperature using the Flory-Huggins theory. Drug Dev Ind Pharm. 2013;39:102–8.
22. Rubinstein M, Colby RH. Polymer physics. 1st ed. New York, USA: Oxford University Press; 2003.
23. van Krevelen D. Properties of polymers: their estimation and correlation with chemical structure. Amsterdam: Elsevier; 1976.
24. Forster A, Hempenstall J, Tucker I, Rades T. Selection of excipients for melt extrusion with two poorly water-soluble drugs by solubility parameter calculation and thermal analysis. Int J Pharm. 2001;226: 147–61.
25. Tao J, Sun Y, Zhang GGZ, Yu L. Solubility of Small-Molecule Crystals in Polymers: d-Mannitol in PVP, Indomethacin in PVP/VA, and Nifedipine in PVP/VA. Pharm Res. 2009;26:855–64.
26. Thakral S, Thakral NK. Prediction of drug-polymer miscibility through the use of solubility parameter based flory-huggins interaction parameter and the experimental validation: PEG as model polymer. J Pharm Sci. 2013;102:2254–63.
27. Young RJ, Lovell PA. Introduction to polymers. 2nd ed. London: Chapman & Hall; 1991.
28. Gupta J, Nunes C, Vyas S, Jonnalagadda S. Prediction of Solubility Parameters and Miscibility of Pharmaceutical Compounds by Molecular Dynamics Simulations. J Phys Chem B. 2011;115:2014–23.
29. Marsac PJ, Konno H, Taylor LS. A comparison of the physical stability of amorphous felodipine and nifedipine systems. Pharm Res. 2006;23:2306–16.
30. Coleman N, Craig D. Modulated temperature differential scanning calorimetry: A novel approach to pharmaceutical thermal analysis. Int J Pharm. 1996;135:13–29.
31. Kestur US, Lee H, Santiago D, Rinaldi C, Won Y, Taylor LS. Effects of the molecular weight and concentration of polymer additives, and temperature on the melt crystallization kinetics of a small drug molecule. Cryst Growth Des. 2010;10:3585–95.
32. Baird JA, Taylor LS. Evaluation of amorphous solid dispersion properties using thermal analysis techniques. Adv Drug Deliv Rev. 2012;64:396–421.
33. Keen JM, Martin C, Machado A, Sandhu H, McGinity JW, DiNunzio JC. Investigation of process temperature and screw speed on properties of a pharmaceutical solid dispersion using corotating and counter-rotating twin-screw extruders. J Pharm Pharmacol. 2014;66:204–17.
34. F. Qian, J. Huang, M.A. Hussain, Drug-Polymer Solubility and Miscibility: Stability Consideration and Practical Challenges in Amorphous Solid Dispersion Development, J. Pharm. Sci. 99 (2010).
35. Gramaglia D, Conway B, Kett V, Malcolm R, Batchelor H. High speed DSC (hyper-DSC) as a tool to measure the solubility of a drug within a solid or semi-solid matrix. Int J Pharm. 2005;301:1–5.
36. Al-Obaidi H, Lawrence MJ, Al-Saden N, Ke P. Investigation of griseofulvin and hydroxypropylmethyl cellulose acetate succinate miscibility in ball milled solid dispersions. Int J Pharm. 2013;443: 95–102.
37. Mohan R, Lorenz H, Myerson A. Solubility measurement using differential scanning calorimetry. Ind Eng Chem Res. 2002;41: 4854–62.
38. Pijpers TFJ, Mathot VBF, Goderis B, Scherrenberg RL. van der Vegte, Eric W., High speed calorimetry for the study of kinetics of (de)vitrification, crystallization, and melting of macromolecules. Macromolecules. 2002;35:3601–13.
39. TANAKA H, NISHI T. Local Phase-Separation at the Growth Front of a Polymer Spherulite during Crystallization and Nonlinear Spherulitic Growth in a Polymer Mixture with a Phase-Diagram. Phys Rev a. 1989;39:783–94.
40. TANAKA H, NISHI T. New Types of Phase-Separation Behavior during the Crystallization Process in Polymer Blends with Phase-Diagram. Phys Rev Lett. 1985;55:1102–5.